Bio-Molecular and Cellular Detection Using SPR Sensor and All-Transparent Microfluidic Platform

Kin Fong Lei[1], Wing Cheung Law[2], Yick-Keung Suen[3],
Wen J. Li[1,*], Ho Pui Ho[2,#], Chinlon Lin[2], and Siu-Kai Kong[3,+]

[1]Centre for Micro and Nano Systems
Faculty of Engineering

[2]Center for Advanced Research
in Photonics
Faculty of Engineering

[3]Department of Biochemistry
Faculty of Science

The Chinese University of Hong Kong, Hong Kong SAR

Abstract - **This paper reports an automated polymer based microfluidic analysis system integrated with a surface plasmon resonance (SPR) biosensor for detecting the specific binding of biomolecules and qualitatively monitoring of cell adhesion on the sensor surface. Micropumps, microchannels, and a SPR biosensor were integrated into a single polymer (PMMA) based microfluidic system. Because SPR based bio-detection requires optically transparent substrates, PMMA is a potential replacement for glass and silicon-glass microfluidic systems, if bio-compatibility and low-cost are desired. The integrated system has been studied for its potential applications in bio-molecules detection and drug-discovery. Two experiments, 1) monitoring the reaction between BSA-BSA antibody, and 2) monitoring the activities of living cells in the presence or absence of trypsin in RPMI-1640 medium, were conducted to show its biomedical applications. The experimental setup and results of these tests are presented in this paper.**

Index Terms – **Microfluidic System, SPR Sensor, Bio-molecular Detection, Cellular Detection.**

I. INTRODUCTION

Research on microfluidics involves the development of miniaturized devices, miniaturized systems, and applications related to the handling of fluids. Over the past ten years, microfluidic lab-on-chip system has been rapidly developed from early single channel devices [1] to current complex analysis systems [2]. The rapid growth of this field is partly due to the rapid developments in MEMS devices, such as micropumps, micromixers, and biosensors, as well as the need for high throughput biomedical analysis and drug delivery system. New generations of automated microfluidic devices have made it possible to achieve biomedical instruments with new levels of performance and capability. Moreover, in the area of biosensors, surface plasmon resonance (SPR) has become a leading technology in biological and chemical sensing because of its real-time and label-free detection capabilities for bio-molecules [3]. Recently, we have proposed a new SPR biosensor design based on measuring the differential optical phase between the *s* and *p* polarizations [4]. The new technique offers a better sensitivity because of its effectiveness in minimizing common-mode noise through the use of differential measurement.

In this paper, a fully automated microfluidic system integrated with a phase-sensitive SPR biosensor is presented. The system consists of three vortex micropumps [5] and a SPR biosensor head [4]. The entire microfluidic system can be fabricated using a low-cost micro-molding replication technique. The working principal of the vortex micropump is based on the vortex flow generation inside the pump chamber by an SU-8 fabricated micro impeller. From our pervious experiments, the vortex micropump can generate a flow rate from 0.11 to 9.5ml/min at an applied voltage from 0.6 to 2.5V with linear relationship. Integrating three vortex micropumps and a SPR biosensor into a single chip, an automated fluid manipulation and bio-detection system can be achieved. The micropumps are software-controlled to pump different solutions sequentially into the SPR biosensor head. For the SPR sensor, results from our pervious work [4] using glycerin-water mixtures indicate that the sensitivity limit of our design can be as high as 5.5×10^{-8} refractive-index units. Such an improvement in the sensitivity limit should put SPR biosensors as a possible replacement of conventional biosensing techniques that are based on fluorescence. We have used our experimental setup, which has real-time phase extraction and software control capabilities, to monitor the binding of the bovine serum albumin (BSA) with BSA antibodies and cell adhesion properties under the influence of trypsin.

II. EXPERIMENTAL SETUP

2.1. Surface Plasmon Resonance

A prism-coupled Kretschmann scheme depicted in Fig. 1 is often used in SPR sensor system. The surface plasmon wave (SPW) vector (k_{sp}) between the metal and dielectric medium can be expressed as:

$$k_{sp} = k_o \sqrt{\frac{\varepsilon_{metal}\varepsilon_{sample}}{\varepsilon_{metal} + \varepsilon_{sample}}} \tag{1}$$

where k_o is the free space wave vector of the optical wave, $\varepsilon_{\text{metal}}$ and $\varepsilon_{\text{sample}}$ are the complex dielectric constants of the metal and the sample medium respectively. The enhanced wave vector of incident light (k_x) is given by:

$$k_x = k_o n_{glass} \sin\theta_{inc} \tag{2}$$

where n_{glass} is the refractive index of the prism, θ_{inc} the angle of incidence. For SPR to take place, which leads to the strongest SPW, the two vectors should be matched. i.e.

*For questions pertaining to microfluidic transport automation: wen@acae.cuhk.edu.hk; #for questions pertaining to SPR detection: hpho@ee.cuhk.edu.hk; +for questions pertaining to bio-molecule and cellular analyses: skkong@cuhk.edu.hk. This project is funded by the Hong Kong Research Grants Council (No. CUHK 4215/01E) and by a CUHK Direct Grant (No.2050305). Wen J. Li is an associate professor at The Chinese University of Hong Kong and also a Distinguished Overseas Scholar of the Chinese Academy of Sciences. Partial support is also provided by the Shenyang Institute of Automation, Chinese Academy of Sciences.

$$k_x = k_{sp} \tag{3}$$

The simplest way to express the phase property of SPR is to use Fresnel equation, the reflection coefficients of the *p*- and *s*-polarized light (r_p and r_s), which are given by [7]:

$$r_p = |r_p| e^{i\phi_p} \text{ and } r_s = |r_s| e^{i\phi_s} \tag{4}$$

Across the resonant peak, the phase angle will exhibit a steep change, which means that a small variation of ε_{sample} or refractive index of sample will lead to a large phase change in the reflected light. Due to the fact that SPR effect will only affect *p*-polarized light, the value of phase different ($\Delta\phi$) between *p*-polarization and *s*-polarization ($\phi_p - \phi_s$) can be used as a refractive index probe on the sensor surface (for detailed explanation, see ref [4]).

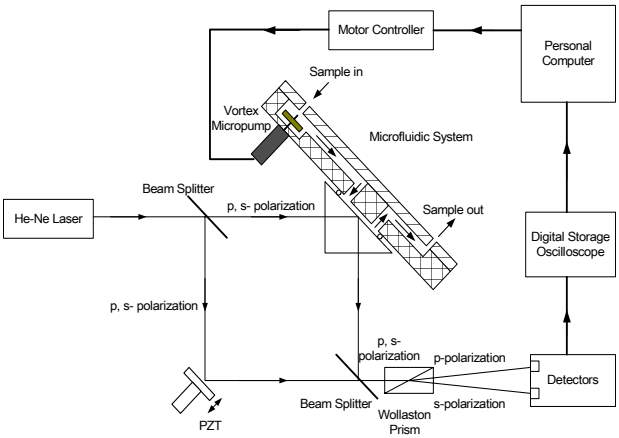

Fig. 1. Experimental setup of the microfluidic system integrated with the SPR biosensor.

2.2. Microfluidic pump

In our automated microfluidic system, fluid flow is driven by vortex micropumps. Detailed fabrication and modeling results developed by our group have been presented in ref [5][6]. The vortex micropump uses kinetic energy to move fluid through the use of an impeller and a circular pump chamber. The basic design concept is illustrated in Fig. 2. As fluid enters the pump near the center of the impeller, it is moved towards the outer diameter of the pump chamber by the rotating motion of the impeller. The confinement provided by the pump chamber forces the fluid to enter the microchannel and a pumping flow is thus created. Since the generation of pumping flow is due to the rotating motion of the impeller, the pumping flow rate can be controlled smoothly by changing the rotational speed of the impeller. This allows digitally controlled fluidic manipulation through straightforward control software.

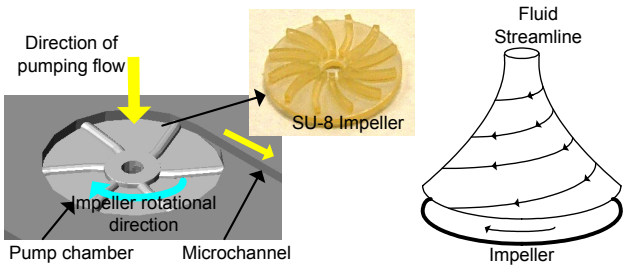

Fig. 2. (a) Illustration of the vortex micropump working principle. (b) Fluid streamline inside the pump chamber.

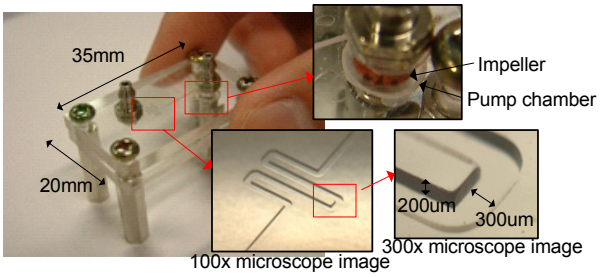

Fig. 3. Photo of a vortex micropump with microchannel. The chip size is 20mm × 35mm. The diameter of pump chamber is 5mm. The output microchannel is 300μm in width, 200μm in depth.

As mentioned earlier, microfluidic systems are required to be optically transparent and bio-compatible for bio-optical detection and chemical applications. For our vortex micropump, we choose polymethyl methacrylate (PMMA) to be the structural material. The SU-8 micro impeller is placed inside the pump chamber. When the fluid enters the micropump from the center of impeller, the rotational motion of impeller, driven by a DC motor, can induce a fluid pressure gradient and thus create a continuous flow. In our vortex pump design, two structural layers are needed. The lower layer includes pump chamber and microchannel, while the upper layer is a cover layer providing fluidic connection. A completed vortex micropump with microchannel is shown in Fig. 3. The diameter of pump chamber is 5mm. The fluid is pumped through an output microchannel of 300μm in width and 200μm in depth.

Experimental and simulation results on the flow rate as a function of rotational speed of the impeller are shown in Fig. 4. The pump performance of two different sizes of the pump chamber, which are 3mm and 5mm in diameter, feeding identical output microchannels are also compared. Our results confirm that the fluid flow rate is proportional to the impeller rotational speed. This also means that the flow rate increase linearly with the DC voltage applied to the motor. From the comparison between two different pump chamber sizes, we found that the larger pump chamber can produce higher fluid flow rate and pressure level. Our experimental data shows that the range of the pump rate is from 0.11ml/min to 9.5ml/min. We have derived an analytical model to approximate the vortex pump performance using the Hagen-Poiseuille equations [6]. The simulation results are compared to experimental results in Fig. 4.

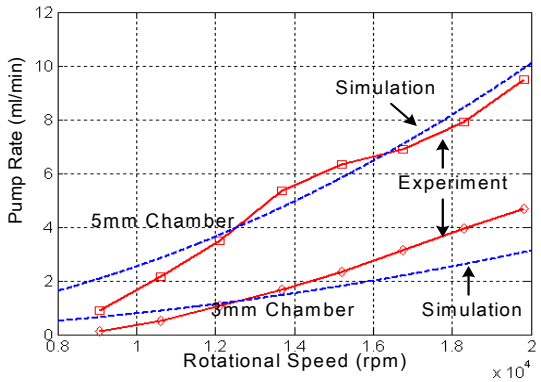

Fig. 4. Comparison of the experimental (solid line) and simulation (dotted line) results. Pump rate (water as pump medium) as a function of rotational speed of impeller.

2.3 Integrated microfluidic system

The experimental setup of the microfluidic system is illustrated in Fig. 1. Three vortex micropumps and a SPR biosensor are integrated into a polymer-based single chip with a computer to control the flow sequence and analyse the SPR signals in a real time manner. In this setup, three different solutions can be pumped into the SPR biosensor head independently. A Mach-Zehnder interferometer with a 10mW polarized He-Ne laser operating at 632.8nm is used as the light source. The polarization direction of the output beam is tuned at 30° from *p*-polarization so that a larger amount of light intensity can be contributed to *p*-polarization to enhance the signal-to-noise ratio of the probe beam. For the sensor head, we use a nominally 45nm gold-coated glass plate attached to a 60° equilateral prism made from BASF10 glass using matching oil. The first 50:50 beam splitter divides the laser into two halves. One beam (probe beam) goes to the sensor head while the beam (reference beam) goes to the plane mirror. A piezoelectric transducer (PZT) is attached to the back of the mirror and a saw-tooth wave oscillating at 120Hz is used to provide the phase modulation signal required by the phase measurement software. Constructive and destructive interferences occurred periodically as a time-varying path difference are introduced by the back-and-forth movement of the mirror. The probe beam and reference beam are combined again at the second beam splitter. In the output beam *p*- and *s*-polarization light are separated by the use of Wollaston prism. Two detectors together with a digital oscilloscope are used to capture the signal and finally the differential phase quantity is extracted. Our experimental setup and the microfluidic system are shown in Fig. 5.

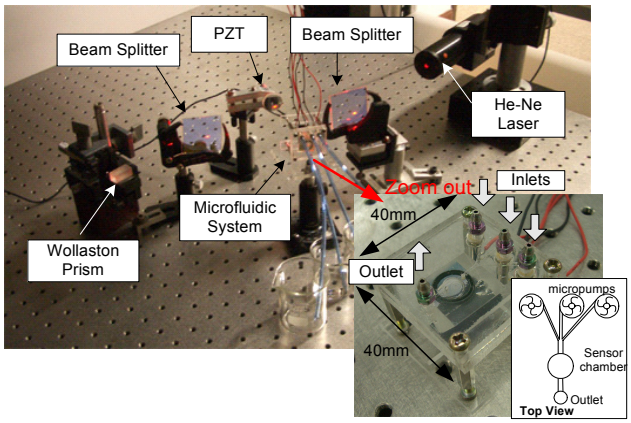

Fig. 5. Experimental setup of the automated microfluidic system integrated with the SPR biosensor for micro cellular detection. A photo (insert) of the polymer based microfluidic system integrated with SPR biosensor. The size of the whole chip is 40mm x 40mm. There are three independent inlets for three different solutions.

III. EXPERIMENT

3.1 Detection of specific binding of biomolecules

In the experiment on biomolecule detection, three types of fluids, namely the buffer, probe and sample fluids were independently introduced into the sensor head. The process sequence is illustrated in Fig. 6. The buffer pump first injected a volume of phosphate-buffered saline (PBS) into the sensor head and the differential phase angle was measured as the baseline. A PBS buffer containing bovine serum albumin (BSA) (1mg/ml)

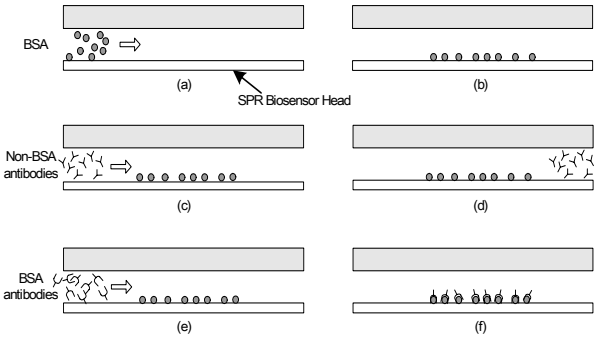

Fig. 6. Illustration of detecting specific binding of antibodies. (a) Injection of BSA. (b) Forming a layer of BSA on the sensor head. (c) Injection of nonspecific BSA antibodies (Rat IgG). (d) Removal of non-specific antibodies without any binding. (e) Injection of specific BSA antibodies. (f) Specific binding of BSA antibodies to BSA.

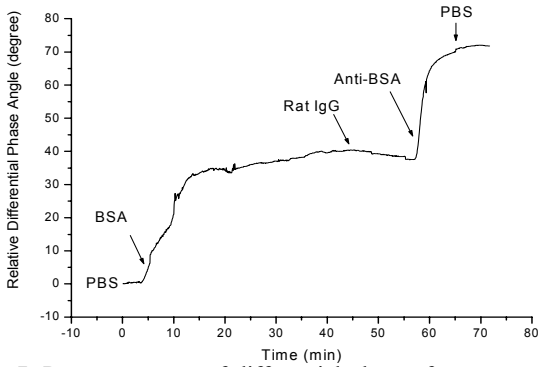

Fig. 7. Response curve of differential phase after sequential addition of PBS, BSA, nonspecific BSA antibody (Rat IgG), and BSA antibody into the sensor head, demonstrating the detection of specific BSA-anti-BSA binding.

was then introduced by the probe pump into the sensor head. As shown in Fig. 7, the phase angle increased upon the addition of BSA-molecules indicating the binding of BSA onto the gold surface. The system was left to settle for 30mins to allow the formation of a BSA layer on the gold surface. A PBS buffer was then injected by the buffer pump into the sensor head again to wash away the free BSA. Then, a PBS buffer containing non-BSA antibodies (Rat IgG) was injected by the sample pump into the sensor head to test whether there was any nonspecific binding. The differential phase remained constant afterward, thus confirming that no nonspecific binding had taken place. PBS buffer containing BSA specific antibodies was then pumped into the sensor head using the sample pump. A sharp increase in phase angle was observed, indicating the binding reaction of BSA with the BSA antibodies. An exponential curve characteristic to typical rate-dependent reactions was also noticed. Since a concentration of 37μg/ml of BSA corresponds to an absolute phase change of 34.4°, we estimate that the detection sensitivity of our setup is 10.76ng/ml (based on 0.01° resolution). Finally, PBS was injected again. The phase angle remained constant, which shows that the sensor surface has been fully covered by BSA antibodies due to the specific binding reaction and the additional BSA antibodies could not find any space on the sensor surface to bind to.

3.2 Cell detachment by trypsin treatment

3.2.1 Material

The cells that we used in our experiment were mouse L929 cell (4 x 10^6 cells/ml) obtained from ATCC (American Type Culture Collection). Prior to the experiment, the mouse cells were put in a rich nutrition buffer, RPMI Medium 1640 from Invitrogen Corporation. RPMI (Roswell Park Memorial Institute) Medium 1640 are liquid medium with enriched formulations for culturing living mammalian cells [8]. With the aid of RPMI, living L929 cells will naturally attach to the gold surface. Trypsin-EDTA (0.25% Trypsin) obtained from Invitrogen Corporation is a common reagent used to remove and detach cells from culture substratum. Trypsin was thus used in our experiment to detach the cells from the gold surface by breaking the adhesion proteins between the cell and the gold surface.

3.2.2 Results

The process sequence is illustrated in Fig. 8. Mouse L929 cells (4 x 10^6 cells/ml) were first cultured on a 45nm gold-coated glass plate at 37°C for two hours. Then the gold surface was observed under an optical microscope to ensure cells were well adhered to the glass plate. As shown in the in-set of Fig. 9, cells were adhered on the gold surface as a monolayer. This glass plate was then attached to a prism using matching oil for phase-sensitive SPR bio-sensing studies. RPMI Medium 1640 was first flowed into the chamber to measure differential phase as a baseline. Trypsin-EDTA (0.25% Trypsin) was then injected into the sensor head. As shown in Fig. 9, an exponential decay curve was observed indicating that the cells were detached from the gold surface. Finally, RPMI was circulated to ensure all the cells were washed out. Another set of control experiment was carried out by repeating the experiment with bare gold glass plate. Only a small phase angle changed was observed when trypsin is added. Thus, we conclude that the large phase change

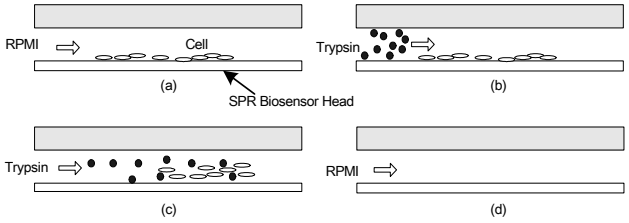

Fig. 8. Illustration of detecting of cell detachment. (a) Injection of RPMI. (b) Injection of trypsin. (c) Detaching cell from the sensor head. (d) No cell left on the sensor surface.

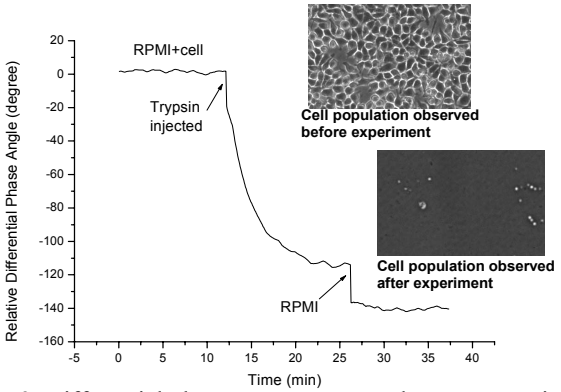

Fig. 9. Differential phase response curve due to sequential addition of RPMI containing cells, trypsin, and RPMI into sensor head.

observed in Fig. 9 must be largely caused by cells detachment. At the end of the experiment, the glass plate was taken out from the prism and observed again under an optical microscope. Visual inspection confirmed that almost all the cells were removed from the surface. Our results show that one can monitor cell detachment affinities using SPR. This is a very useful platform for a range of biomedical applications e.g. drug discovery by simply replacing trypsin with newly invented drugs.

IV. CONCLUSION

Detection of bio-specific protein partners (BSA and BSA-antibody) and monitoring of cell activities have been successfully demonstrated using our new SPR biosensor integrated with an automated microfluidic system. This preliminary study on cell activity showed the possibilities of using differential phase SPR bio-sensors in a wide range of biomedical applications. Our integrated system will provide a useful platform for high-throughput diagnostic tests on cells and biomolecules at a very low cost. Furthermore, arrayed sensing surface with multiple analytes and parallel detection by using a 2-D phase imaging technique will certainly be a very exciting direction for further development of phase-sensitive SPR sensors.

ACKNOWLEDGEMENT

The authors wish to thank The Chinese University of Hong Kong for providing research studentships to W.C. Law. Funding support from a CUHK Direct grant under Project #2050305 and from a HKRGC Grant (CUHK 4215/01E) are also gratefully acknowledged.

REFERENCES

[1] D. J. Harrison, K. Fluri, K. Seiler, Z. Fan, C. S. Effenhauser and A. Manz, "Micromachining a Miniaturized Capillary Electrophoresis-based Chemical Analysis System on a Chip", *Science* 261, pp.895-897, 1993.

[2] M. J. Powers, K. Domansky, M. R. Kaazempur-Mofrad, A. Kalezi, A. Capitano, A. Upadhyaya, P. Kurzawski, K. E. Wack, D. B. Stolz, R. Kamm and L. G. Griffith, "A Microfabricated Array Bioreactor for Perfused 3D Liver Culture", *Biotechnol. Bioeng.* 78, pp.257-269, 2002.

[3] J. Melendez, R. Carr, D. U. Bartholomew, K. Kukanskis, J. Elkind, S. Yee, C. Furlong and R. Woodbury, "A commercial solution for surface plasmon sensing", *Sensors and Actuators*, B 35, pp.212-216, 1996.

[4] S. Y. Wu, H. P. Ho, W. C. Law, C. Lin and S. K. Kong, "Highly Sensitive Differential Phase-sensitive Surface Plasmon Resonance Biosensor Based on the Mach-Zehnder Configuration", *Optics Letters*, vol. 29, no. 20, pp.2378-2380, March 2004.

[5] K. F. Lei and Wen J. Li, "Microfluidic Mixing by Fluidic Discretization", accepted, 13th International Conference on Solid-State Sensors, Actuators, and Microsystems, (*Transducers 2005),* Jun 05-09 2005, Korea.

[6] K. F. Lei, W. J. Li and Y. Yam, "Fabrication, Modeling, and Experimental Analysis of a Novel Vortex Micropump for Applications in PMMA-Based Micro Fluidic Systems", submitted, *Journal of Micromechanics and Microengineering*, Institute of Physics, U. K., 2005.

[7] P. Yeh, *Optical Waves in Layered Media*, Wiley, New York, 1988.

[8] Invitrogen Catalog, Invitrogen Corporation. www.invitrogen.com.